Capillary Electrophoresis and Sample Injection Systems Integrated on a Planar Glass Chip

D. Jed Harrison,*,†,‡ Andreas Manz,*,§ Zhonghui Fan,‡ Hans Lüdi,§ and H. Michael Widmer§

Department of Chemistry, University of Alberta, Edmonton, Alberta, Canada T6G 2G2, and Forschung Analytik, Ciba Geigy, CH 4002 Basel, Switzerland

The feasibility of miniaturizing a chemical analysis system on a planar substrate has been demonstrated for a system utilizing electrokinetic phenomena for sample separation and solvent pumping. Using micromachining techniques, a complex manifold of capillary channels has been fabricated in a planar glass substrate and the separation of a mixture of fluorescein and calcein within the channels was achieved using electrophoresis. The maximum number of theoretical plates obtained was about 35 000 for calcein, with 5000 V applied, corresponding to 2100 V between the injection and fluorescence detection points in the channels. The number of theoretical plates observed was in agreement with theory, indicating no interactions between the analyte and the glass walls. The electroosmotic flow rate in the glass channels was $(4.5 \pm 0.1) \times 10^{-4}$ cm²/(V·s) using a pH 8.5 50 mM boric acid, 50 mM Tris buffer, comparable to $(5.87 \pm 0.08) \times 10^{-4}$ cm²/(V·s) measured in fused-silica capillaries. Solvent flow could be directed along a specified capillary by application of appropriate voltages, so that valveless switching of fluid flow between capillaries could be achieved. These results provide a foundation for the design of more complex sample treatment and separation systems integrated on glass or silicon substrates.

Most successful analyses in the laboratory involve a complete *system* of sample treatment, separation, and analysis, designed to circumvent the complexities of a sample and its matrix. These methods are often time consuming or labor intensive. To overcome this, the analysis process may be automated, increasing its speed, precision, and reproducibility. The use of flow injection analysis (FIA), and its coupling to separation methods such as gas or liquid chromatography, or selective chemical sensors is one route to achieve this. High levels of automation have resulted in total chemical analysis systems (TAS) that can be used to monitor chemical concentrations continuously in industrial chemical and biochemical processes.[1-3] The miniaturization of a TAS onto a monolithic structure could produce a device (a μ-TAS) that would resemble a sensor in many ways.[4,5] Such a device could be configured as a dip-type probe, giving out a reading for the analyte of interest, so that it behaved as a sensor from the perspective of the user. Separation methods such as liquid chromatography and capillary electrophoresis, as well as other bench-top analytical approaches such as FIA may also benefit from the μ-TAS approach. It has been made clear that smaller dimensions result in improved performance for these analytical methods.[6-9] The benefits of miniaturization, though, are complicated by problems of detection and dead volumes associated with coupling capillaries to detectors and injectors. Several authors have noted that the use of microlithographic techniques to fabricate systems would be beneficial.[9-11] The ease of fabrication of small structures should facilitate coupling of capillary separation systems to each other for 2-dimensional separations or to injectors and detectors, with minimum dead volume. Increased speed of analysis, decreased sample and solvent consumption, or increased detector efficiency could also be realized, as we have discussed in detail elsewhere.[4,5]

Micromachining of silicon or other planar materials provides a path to development of liquid-phase μ-TAS devices.[12] The combination of microlithiography with isotropic and anisotropic etching techniques, as well as controlled thin-film deposition, allows for the fabrication of micron-scale, 3-dimensional structures.[13-18] Terry et al.[13] developed a gas chromatograph on a silicon wafer, but there have been relatively few extensions of this technology to solution-phase systems. Bergveld's group has designed micron-scale coulometric titration systems,[19] and Shoji et al.[20] have developed a dissolved O_2 sensor based on a micromachined device. Both of these systems are based on the pH-sensitive field effect transistor (pH FET) but, because of their integrated system approach, offer better performance than the stand-alone pH FET does. A micromachined liquid chromatograph has been reported and the theoretical behavior of such a system discussed, but no data from the system has been presented.[21]

Capillary electrophoresis (CE) is a separation method that could be coupled with FIA on a planar substrate to explore

* Authors to whom correspondence should be addressed.
† Research performed while on leave at Ciba Geigy, Basel.
‡ University of Alberta.
§ Ciba Geigy.

(1) Graber, N.; Lüdi, H.; Widmer, H. M. *Sens. Actuators* **1990**, *B1*, 239-243.
(2) Gisin, M.; Thommen, C. *Anal. Chim. Acta* **1986**, *190*, 165-176.
(3) Garn, M.; Cevey, P.; Gisin, M.; Thommen, C. *Biotechnol. Bioeng.* **1989**, *34*, 423-428.
(4) Manz, A.; Graber, N.; Widmer, H. M. *Sens. Actuators* **1990**, *B1*, 244-248.
(5) Manz, A.; Fettinger, J. C.; Verpoorte, E.; Lüdi, H.; Widmer, H. M.; Harrison, D. J. *Trends Anal. Chem.* **1991**, *10*, 144-149.
(6) *Small Bore Liquid Chromatography Columns: Their Properties and Uses*; Scott, R. P. W., Ed.; Wiley: New York, 1984.
(7) *Micro-Column High Performance Liquid Chromatography*; Kucera, P., Ed.; Elsevier: Amsterdam, 1984.
(8) Microcolumn Separations: Columns, Instrumentation and Ancillary Techniques. *J. Chromatog. Libr.* **1985**, *30*.
(9) van der Linden, W. E. *Trends Anal. Chem.* **1987**, *6*, 37-40.
(10) Ruzicka, J.; Hansen, E. H. *Anal. Chem. Acta* **1984**, *161*, 1-10.
(11) Monnig, C. A.; Jorgenson, J. W. *Anal. Chem.* **1991**, *63*, 802-807.
(12) Petersen, K. E. *Proc. IEEE* **1982**, *70*, 420-457.
(13) Terry, S. C.; Jermon, J. H.; Angell, J. B. *IEEE Trans. Electron. Devices* **1979**, *ED-26*, 1880-1886.
(14) Muller, R. S. *Sens. Actuators* **1990**, *A21*, 1-8.
(15) Esashi, M.; Shoji, S.; Nakano, A. *Sens. Actuators* **1989**, *20*, 163-169.
(16) Fan, L.-S.; Tai, Y.-C.; Muller, R. S. *IEEE Trans. Electron. Devices* **1988**, *ED-35*, 724-730.
(17) Sato, K.; Kawamura, Y.; Tanaka, S.; Uchida, K.; Kohida, H. *Sens. Actuators* **1990**, *A21*, 948-953.
(18) Kittisland, G.; Stemme, G.; Norden, B. *Sens. Actuators* **1990**, *A21*, 904-907.
(19) Olthus, W.; van der Schoot, B. H.; Bergveld, P. *Sens. Actuators* **1989**, *17*, 279-283.
(20) Shoji, S.; Esashi, M.; Matsuo, T. *Sens. Actuators* **1988**, *14*, 101-107.
(21) Manz, A.; Miyahara, Y.; Miura, J.; Watanabe, Y.; Miyagi, H.; Sato, K. *Sens. Actuators* **1990**, *B1*, 249-255.

0003-2700/92/0364-1926$03.00/0

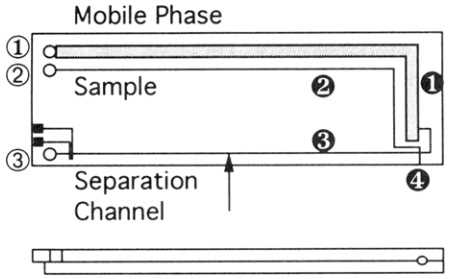

Figure 1. Layout of the channels in a planar glass substrate. Channels referred to in the text are identified by number (filled circles), as are the inlet points (reservoirs) to each channel (open circles). Each channel is labeled with its content or its function. Overall dimensions are 14.8 cm × 3.9 cm × 1 cm thick. The location of one pair of Pt electrodes is also shown; for clarity the others are not. The point of fluorescence detection is marked by an arrow.

the μ-TAS concept, and this paper examines the feasibility of doing so. There are several reasons for selecting this combination of methods.[5,22] FIA, of course, provides a convenient means of automating sample workup prior to injection into a separation system or detector coil. Capillary electrophoresis, in which the driving force is an electric field, has proven to be a powerful separation method.[23] There are two phenomena involved: the solvent and solutes all migrate due to electroosmotic motion of the solvent, which is generated within the Helmholtz layer near the usually negatively charged walls of the capillary, while the ions are additionally driven by migration in the electric field. The ions are separated due to the differences in their electrophoretic mobilities (migration rates). The electroosmotic flow rate is usually larger than that of electrophoretic migration, so that all the sample moves in one direction. Because of electroosmotic flow, applied voltages may be used to pump fluid in a flow injection pretreatment system, as well as to induce separation in a coupled electrophoresis capillary. Electroosmotic pumping is well suited to the μ-TAS concept, since the flow rate of solvent is controlled by electrokinetic effects that are approximately independent of capillary dimensions. In contrast, methods utilizing more conventional pumps develop extremely high back-pressures with small capillary dimensions and are not well suited to delivery of such low volumes.[4,5]

By micromachining a complex manifold of flow channels in a planar substrate, it is possible to fabricate a network of capillaries capable of sample injection, pretreatment, and separation. We have recently described the design of such a system.[5] To understand what factors play a role in the performance of such a device, it is useful to consider here the modes of operation envisioned to effect an analysis. Figure 1 shows a layout of a simple device for sample injection and separation that has been fabricated to test the concepts discussed above. It consists of inlets, or reservoirs, at the heads of three interconnected capillary channels. An inlet to a fourth channel is located near the intersection of the channels. As conceived, the application of a voltage between any two inlets should cause electroosmotic pumping of fluid along those channel segments between the inlets. Valveless switching of fluid flow between channels should be achieved by switching the voltages applied to each channel. For example, voltage applied between inlets 2 and 4 should draw sample into the channel and past the intersection point. Subsequent application of a voltage between inlets 1 and 3 should then drive a small plug of sample along channel 3, effecting electrophoretic separation of the sample plug.

In this work we have demonstrated the feasibility of using electroosmotic pumping and electrophoretic separation methods within a planar structure fabricated in glass. The effectiveness of the glass substrate for electrophoretic separation has been compared to more conventional fused-silica capillaries. In addition, the valveless switching of fluid flow between channels in a multichannel manifold has been studied and the limits of the approach explored. The results show that the combination of FIA and CE in a μ-TAS environment is possible, opening up exciting possibilities for this approach.

EXPERIMENTAL SECTION

Reagents. Two buffer solutions made from reagent grade chemicals were used for electrophoresis: a pH 8.5 buffer, 0.050 M in boric acid, 0.050 M in tris(hydroxymethyl)amino methane (Tris), adjusted with Tris to pH 8.5, and a pH 7.0 phosphate buffer, 0.041 M Na_2HPO_4, 0.028 M KH_2PO_4, adjusted with HCl or NaOH. Stock solutions of 100 μM fluorescein and calcein (chromatographically purified, Molecular Probes, Inc., Eugene, Or) in pH 8.5 buffer, with about 3% methanol added, were used to prepare 10 and 20 μM solutions of the dyes.

Devices. The glass structures were fabricated under contract by Mettler AG (Switzerland) using their proprietary lithographic process. In general this process involves masking a glass substrate with a metal layer, followed by lithographic patterning of the metal mask.[5] The exposed glass is then etched with an HF-based solution to produce channels in the glass, and the mask is then removed. As mentioned, this process is commercially available. In this report one 5-mm-thick glass plate had channels etched in it to a 10-μm depth, while the 5-mm-thick cover plate had Pt metal electrodes defined on it. The 20-μm-wide Pt leads were defined in pairs separated by 20 μm within the channel, with 1-mm-wide contact leads running out to contact pads near the three inlet reservoirs. Three holes were made through the top plate to contact three of the channels and form a small reservoir, as indicated in Figure 1. A fourth inlet was formed on the edge of the device, where the two plates bonded, simply by etching one of the narrow channels out to the edge of the plate. The top and bottom glass plates of each device were bonded together by melting under controlled conditions. Steel weights were placed on the top plate and the two plates were then heated in a muffle furnace at 500 °C for 1 h, 550 °C for 0.5 h, and 620 °C for about 2 h, before cooling to 550 °C for 1 h. The furnace was then turned off, and the structures were allowed to cool inside overnight. Frequently, some regions were not properly bonded, and the cycle was repeated, with weights placed over these regions.

Measurement Methods. FUG Elektronik Model HCN 2000 and 12 500 power supplies (Rosenhein, Germany) were used for the electrophoresis experiments. Their current-monitoring sensitivity was insufficient, so current in the electrophoresis channel was monitored by the voltage drop across a 10-kΩ resistor placed between one solvent reservoir and ground. The voltage drop was recorded with a Phillips dual-pen strip chart recorder. For measurement of current-voltage curves the power supplies were ramped in time by external programming using a Compaq 386 system equipped with a Metrabyte DDA 06 digital-to-analog converter. The software package ASYST (Kiethly) provided the programming environment. For electrophoresis experiments the power supply potential was set manually.

A 488-nm air-cooled, Ar ion laser (Spectra Physics, 161C-9) operated at 4 mW served as a fluorescence excitation source.[24,25] It was focused into an optical fiber, the outlet of which was mounted immediately above the channel in which sample was to be detected. A fiber optic collection bundle was mounted above the channel at 45° to the incident light. This was coupled to a sealed photomultiplier tube (PMT) housing. A pair of Omega 530 DF 8907 and Schott OG515 optical filters were placed between the bundle and the Centronics 4249B PMT, to eliminate scattered laser light and most of the room light. The PMT current was amplified with a battery-powered UDT Model 101C transim-

(22) Gale, R. J.; Ghowsi, K. In *Biosensor Technology, Fundamentals and Applications*; Buck, R. P., Hatfield, W. E., Umana, M., Bowder, E. F., Eds.; Marcel Dekker: New York, 1990; pp 55–62.

(23) Ewing, A. G.; Wallingford, R. A.; Olefirowicz, T. M. *Anal. Chem.* **1989**, *61*, 292A–294A.

(24) Zare, R. N.; Gassmann, E. Eur. Pat. Appl. EP 216600, 1987.

(25) Cheng, Y-F.; Dovichi, N. J. *Science* **1988**, *242*, 562–564.

pedance amplifier, and the signal was recorded with a Phillips dual-pen strip chart recorder. The glass structure was mounted on an $x-y$ translation stage to allow fine positioning adjustments. The detection point was 6.5 cm from the intersection point along channel 3 (see Figure 1).

A Spectra Physics electrophoresis unit equipped with an absorbance detector was used for conventional capillary electrophoresis measurements. A 45-cm-long, 75-μm-i.d. fused-silica capillary was used with a total applied voltage of 14.8 kV. The distance to the detector was 38 cm. The pH 8.5 boric acid, Tris buffer was used and a current of 15 μA was obtained. Sample was injected over a 1-s period by a hydrodynamic method. Sample concentrations were 10^{-4} M.

The diffusion coefficient of 1 mM fluorescein in pH 8.5 buffer was determined from the diffusion-limited reduction current[26] obtained at a dropping-Hg electrode. The rate of flow of Hg from the capillary was measured in the same solution, so that the diffusion coefficient could be calculated using the Ilkovic equation.

The potential of electrodes in the channels of the glass device was measured relative to ground with a Burr-Brown Model 3584JM high-voltage operational amplifier. The amplifier was configured as a voltage follower and was supplied with +115 V relative to ground.

Procedures. Solutions were introduced into the channels via the 3-mm-diameter reservoirs at the ends of the channels using a syringe. A disposable plastic pipet tip was cut to fit the syringe and the reservoir, to allow application of modest pressures. Some care was taken to avoid trapping air inside. Fluorescent dye solutions were introduced through reservoir 2 by syringe and then driven in or out of channel 3 by application of a voltage between reservoirs 2 and 3. The fluorescence detector was aligned to channel 3 with dye present in the channel.

Plastic pipet tips were inserted in the three reservoirs and filled with solutions to a height of about 1 cm above the device. Fine Pt wires were inserted in the reservoirs to supply the electrophoresis voltage.

RESULTS AND DISCUSSION

Figure 1 shows the layout of the glass device. Separations were performed in channel 3, while sample was introduced through channel 2 and mobile phase through channel 1. The dimensions of the capillary channels were designed to produce a minimum potential drop in channel 1, which supplies the mobile phase before the sample injection point. To effect this, channels 2 and 3 were made narrow, 30 μm wide and 10 μm deep, while channel 1 was 1 mm wide and 10 μm deep. The device was fabricated from an upper and lower plate, one with the channels etched in it, the other with Pt electrodes deposited. The Pt electrodes prevented the upper and lower glass plates of the device from contact bonding, and bonding them with optical cement still allowed water to leak between the plates. Consequently, the plates were melted together under carefully determined conditions to prevent the channels from collapsing. Figure 2 shows a photomicrograph of the intersection point of the narrow channels. It can be seen that the melting process used for bonding the plates did not seriously distort the channel shape. It was also observed that the glass had flowed enough to seal the Pt electrodes and prevent leakage.

Unlike the other reservoirs, inlet 4 in Figure 1 was not formed by a hole through the top glass plate. Instead channel 4 was etched out to the edge of the bottom plate, so that a small rectangular hole allowed contact to the external environment. It was originally intended that the structure would be dipped into solution so that inlet 4 would be immersed. This would have allowed rapid electrokinetic injection of sample. However, leaving this point open caused a secondary flow of solvent due either to capillary action drawing solvent out or the effect of hydrostatic pressure differences. Consequently, this inlet was plugged with epoxy and sample was introduced from reservoir 2.

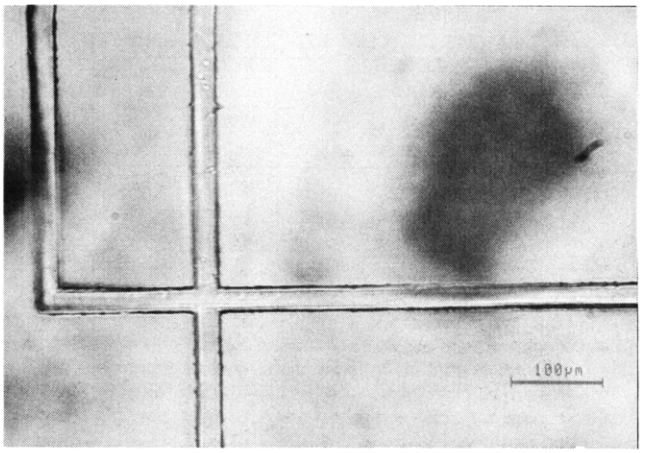

Figure 2. Photomicrograph of the intersection point of the four channels shown in Figure 1 after the glass plates have been bonded together. The channel width is 30 μm.

Electrical Characteristics. Initial characterization of the planar capillary electrophoresis structure involved measurement of the capillary current versus applied voltage ($I-V$) characteristics, and determination of the voltage range at which electrical failure occurred. The voltage was applied between reservoirs 1, 2, or 3; these are identified in Figure 1. The $I-V$ response was linear, with a correlation coefficient of 0.999, for potentials of up to 5000 V applied between any pair of reservoirs. The ratios of the resistances measured between each reservoir were in agreement with the ratios of the channel lengths and cross-sectional areas. The reproducibility of the channel resistance was quite good, varying by ±4% over 2 weeks of measurements. Qualitatively, the resistance is a function of the electrolyte conductivity. For the channel between reservoirs 1 and 3 (channel 1–3) the resistance drops from 7.3 GΩ, when filled with the relatively low conductivity, pH 8.5 boric acid, Tris buffer, to 0.91 GΩ, when filled with a much higher conductance, pH 7.0 phosphate buffer. This behavior was not explored quantitatively. The linearity of the $I-V$ curves and their dependence on channel length and solution conductivity indicate the current flow occurs through the channels. The linearity further shows that the joule heat generated in the channels at these potentials is effectively dissipated.

The potential distribution inside the channels was measured with 96.6 V applied between reservoirs 1 and 3 (3 at ground). A sensing electrode placed in reservoir 2, which should be at the potential of the intersection point of the channels, gave a value of 88.3 V. On the basis of the channel cross-sections and lengths, a potential of 88 V was predicted. This indicates that very little potential drop occurs in the wide channel segment of channel 1, due to the large cross-section over most of the path length. The potentials of three Pt electrodes integrated into channel 3 of the device were also measured. These electrodes, located at distances of 1.2, 70, and 132 mm from the edge of reservoir 3, had potentials of 0.9, 44, and 87.7 V, respectively. These values are within 3% of the predicted values, on the basis of the channel geometries. The good agreement between the predicted and observed potential distribution indicates that the current flow is through the channels. Further, it shows that the impedance of each capillary channel segment can be carefully controlled. Isolation of the Pt electrodes from potentials other than those at the location where they contact the channel is also evidenced. Future work using these electrodes for on-column electrochemical or conductivity detection is planned.

(26) Delahay, P. *Bull. Soc. Chem.* **1948**, *15*, 348–350.

Control of the potential drop within a given channel by control of its cross-sectional area will prove to be an important tool in the design of devices. It will ensure the majority of the potential can be applied in the active separation channel, rather than in the segment that connects to the external reservoir, providing the maximum efficiency of design. This is illustrated by the device shown in Figure 1. Channel 1 was made quite long so that the reservoirs were in a convenient location, but there was no need for a large potential drop in channel 1, since it is located before the sample injection point.

At this stage of testing, when the applied voltage increased above 5 kV the $I-V$ curves became highly nonlinear, with the current increasing from 1 to 20 μA between 6 and 10 kV. Arcing began to occur in this voltage range, although the exact potential usually varied randomly between devices and over time. The location of the arcing sites was not clear, but it appeared to be between reservoirs. Arcing failure sometimes occurred at voltages of 4 kV or less, but this could be remedied by thoroughly washing the device's surface with distilled water and then drying it. Surface contamination with salt solutions is the most likely source of this low-field failure. Very recently we have shown that linear $I-V$ curves can be obtained at potentials up to 25 kV, with no arcing. This work will be described elsewhere, but we note here that attaining these fields required the Pt leads contacting the reservoirs be carefully isolated from each other by placing them inside glass tubing.[27] The minimum distance between reservoirs 1 and 2 is 0.20 cm. Thus, a field of up to 25 kV/cm can be sustained without care to isolate the leads, and much higher values (>100 kV/cm) can be withstood by the glass structure itself.

Electrokinetic Phenomena. To determine whether electrophoretic and electroosmotic flow occurred within the glass channels, a mixture of fluorescein and calcein in pH 8.5 boric acid, Tris buffer was studied. Calcein is a diaminotetraacetic acid derivative of fluorescein that is somewhat larger in size and has a different charge at pH 8.5. Fluorescence detection 6.5 cm from the intersection of the channels was used to monitor the sample in channel 3.[24,25]

Sample was injected by syringe from reservoir 2, and then channel 1–3 was flushed with pH 8.5 buffer using a syringe with reservoir 2 blocked. A positive voltage applied between reservoirs 2 and 3 (3 at ground) caused the sample solution in channel 2 to move into channel 3 and along past the detector. This was evidenced by two stepwise increases of equal magnitude in the fluorescence signal as the dyes migrated along the channel. The first front corresponded to the more mobile sample component, while the second step was seen when the second component front also reached the detector location.

A small plug of sample could be injected from channel 2 into channel 3 at the intersection point by applying a voltage between reservoirs 2 and 3 for a brief period. Application of a positive potential between reservoirs 1 and 3 then drove this plug along channel 3 past the detector. Figure 3 shows the resulting electropherogram for an applied potential of 3000 V, which corresponds to 1260 V between the injection and detection points. The figure demonstrates that electrophoretic separation of the two component mixture occurs, and that the peaks appear nearly Gaussian in shape. The peak heights were proportional to the injection voltage applied between reservoirs 2 and 3, as well as to the length of time it was applied. A detailed study was not made, but the precision was approximately ±20%. Injection of each component separately identified the first peak as calcein and the second as fluorescein, on the basis of their migration times.

(27) K. Seiler, D. J. Harrison, unpublished work.

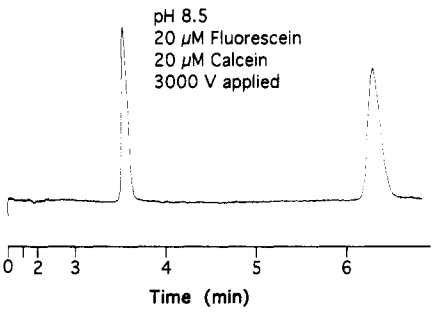

Figure 3. Electropherogram of a sample plug injected from channel 2 into channel 3 with 250 V applied between reservoirs 2 and 3 for 30 s. A voltage of 3000 V was then applied between reservoirs 1 and 3 to effect the separation along channel 1–3. The sample was 20 μM fluorescein, 20 μM calcein, and a pH 8.5 buffer was used. Note the time scale was expanded 2.7 min after sample injection.

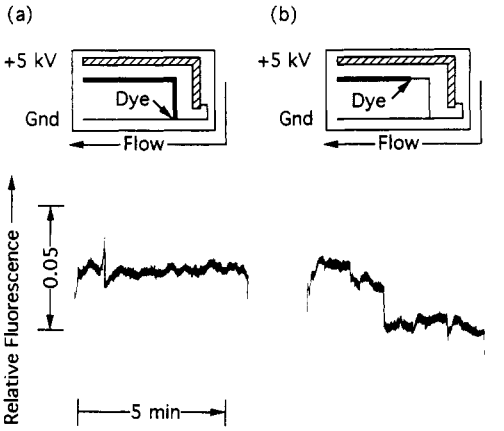

Figure 4. (a) Background fluorescence observed with 5000 V applied between reservoirs 1 and 3 with pH 8.5 buffer in channel 1–3. Initially, 10 μM calcein, 20 μM fluorescein sample was present in channel 2 at the intersection point. (b) The pH 8.5 buffer was then driven back into channel 2 from the intersection to prevent the dye from leaking into channel 1–3 and the background fluorescence was observed with 5000 V reapplied between reservoirs 1 and 3. A decrease in background signal resulted. The fluorescence scale is expressed relative to the signal measured for the calcein, fluorescein mixture.

These results indicate that electrophoretic separation can be achieved using a glass substrate in a planar configuration. Injection and separation of a sample plug from channel 2 also demonstrates that the concept of manipulation of flow patterns selectively within the channel manifold is possible. This is the process of valveless switching discussed above, but its demonstration does not indicate how exclusively the flow is restricted to the intended channel. Consider that once a sample plug was injected from channel 2 into channel 3, sample solution remained in channel 2 at the intersection point. The potential at reservoir 2 was then left floating while a field was applied between reservoirs 1 and 3. Consequently, the sample in channel 2 was free to diffuse into the intersection volume or be pulled in by the convective flow along channel 1–3. This fluid leakage can be expected to limit the effectiveness of the valveless switching concept and could require active control of the potential of each reservoir at all times.

The leakage of fluid from channel 2 into channel 1–3 was evaluated in three steps. In step 1 a 10 μM calcein, 20 μM fluorescein sample at pH 8.5 was present throughout the entire length of channel 2, while pH 8.5 buffer was in the other channels, as indicated in Figure 4a. Then 5000 V was applied between reservoirs 1 and 3 (3 at ground) to drive the pH 8.5 buffer between them, as illustrated by the flow direction marker in Figure 4a. With the dye solution in channel 2 present at and near the intersection of the channels, any

leakage from this channel into channel 1–3 would contaminate the buffer solution moving toward the detector. This would increase the background fluorescence at the detector in channel 3. Figure 4a shows the background fluorescence observed with 5000 V applied to channel 1–3, after the equilibrium signal in the presence of dye at the intersection had been established. In the second step of the experiment the dye solution in channel 2 was driven back from the intersection by applying 5000 V between reservoirs 1 and 2 (2 at ground). As a result a large part of channel 2, including the region near the intersection point, was filled with pH 8.5 buffer rather than the dye solution. At this stage the 6.5-cm-long plug of solution in channel 3 between the intersection point and the detector was still contaminated with dye, as a result of the first step of the experiment. Finally, in the third step, illustrated in Figure 4b, 5000 V was reapplied between reservoirs 1 and 3, to again direct the flow along channel 1–3. Figure 4b also shows how the fluorescence intensity responded. Note that the fluorescence intensity scale in Figure 4 is expressed as the intensity of the observed signal, ratioed to the intensity that would be observed if instead a 10 μM calcein, 20 μM fluorescein solution were driven past the detector. It can be seen that the fluorescence intensity decreased in two steps after 5000 V was reapplied to channel 1–3. These steps correspond to migration of the two contaminants in the 6.5-cm-long plug in channel 3 past the detector, first the calcein (10 μM) and then the more slowly moving fluorescein (20 μM). The decrease in intensity resulted from the fact that any leakage from channel 2 no longer delivered dye into channel 3, since the dye was no longer present at the intersection.

The series of experiments described above indicate some solution was drawn in from channel 2 while solvent flowed along channel 1–3, due to diffusion and/or convective effects. However, the magnitude of the leakage was small, as the change in fluorescence intensity caused by removal of the dye from the intersection with channel 2 was about 3.5% of that seen for introduction of a 10 μM calcein, 20 μM fluorescein solution into channel 3. This level of leakage should be acceptable for many applications, and more complex flow manifolds or control of voltages on the side channels could be used to reduce the leakage for critical applications.

The migration times, t_m, for fluorescein and calcein were determined over an applied voltage range of 1000–5000 V, corresponding to 420–2100 V between the injection point and the detector. The overall mobility, μ, is related to the applied voltage by eq 1,[28,29] where d is the distance from the injection

$$d/t_m = \mu 0.91 V_{ap}/L \quad (1)$$

point to the detector and V_{ap} is the total applied voltage. Since channel 1–3 has two segments of different cross-section, the electric field in the narrow channel is calculated from the fraction (0.91) of V_{ap} that drops between the intersection point and reservoir 3. The length of that segment, L, is 13.9 cm. Plots of $1/t_m$ versus V_{ap} are linear (correlation coefficient of 0.998), giving overall mobilities of (1.90 ± 0.03) and (1.21 ± 0.06) × 10^{-4} $cm^2/(V \cdot s)$ for calcein and fluorescein, respectively. The values and errors reported here and in the following text are the averages and standard deviations of several replicate experiments.

The mobility of fluorescein in pH 8.5 buffer in a conventional fused-silica capillary column equipped with an absorbance detector was found to be (2.59 ± 0.05) × 10^{-4} $cm^2/(V \cdot s)$, and that of the neutral marker tryptophan was (5.87 ± 0.08) × 10^{-4} $cm^2/(V \cdot s)$. Using these data and eq 2, where μ_{ep} is the

$$\mu = \mu_{ep} + \mu_{eo} \quad (2)$$

electrophoretic mobility and μ_{eo} is the electroosmotic mobility, the values of μ_{ep} and μ_{eo} in both the fused-silica capillary and the planar glass channel could be determined. It is assumed that μ_{ep} was the same for fluorescein in the glass and the fused-silica capillaries. The electrophoretic mobilities of calcein and fluorescein in the glass device were found to be (−2.6 ± 0.1) and (−3.3 ± 0.1) × 10^{-4} $cm^2/(V \cdot s)$, respectively. The electroosmotic mobility in the fused-silica column was (5.87 ± 0.08) × 10^{-4} $cm^2/(V \cdot s)$, while in the glass structure it was (4.5 ± 0.1) × 10^{-4} $cm^2/(V \cdot s)$. These values indicate that electroosmotic flow does occur within the glass substrate, and that it has a magnitude similar to that in fused silica.

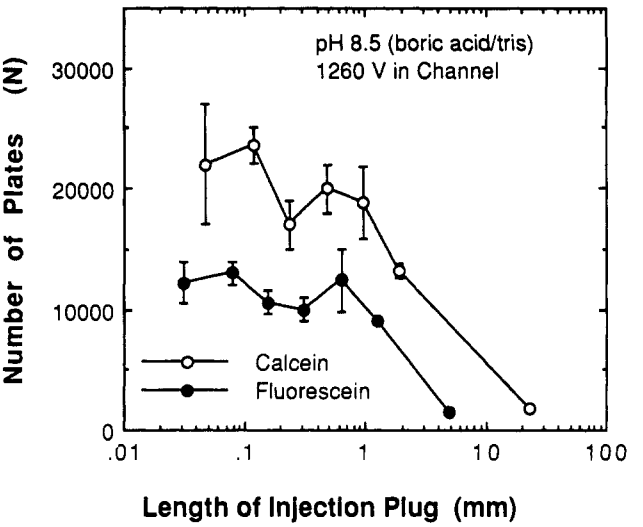

Figure 5. Plot of the number of theoretical plates, N, as a function of the length of sample plug injected from channel 2 into channel 3. 3000 V was applied between reservoirs 1 and 3 (1260 V in the active channel) during the separations of the 20 μM fluorescein, 20 μM calcein samples.

Separation Efficiency. Knowing the value of μ, it was possible to estimate the length of the sample plug electrokinetically injected from channel 2 into channel 3. The separation efficiency, expressed as the number of theoretical plates, N, could then be determined as a function of the size of sample plug injected. Figure 5 shows a plot of N versus the plug length. N was calculated using eq 3,[30] where W_t is

$$N = 8 \ln 2 (t_m/W_t)^2 \quad (3)$$

the full width of the peak at half-maximum, expressed in terms of time. For both compounds, N reaches a plateau when the sample plug length decreases below about 0.6–0.9 mm. This is consistent with the estimated detector cell length of about 0.8–1 mm. The fluorescence detector design was far from optimized and did not incorporate a focusing lens for the laser excitation beam, a collection lens, or a slit to minimize the field of view. In light of this, it is not surprising the detector optics limited the separation efficiency. The results do show that very small sample lengths are readily injected and detected; the minimum volume injected corresponds to 0.8 fmol of dye. Better mass and concentration detection limits should be readily achieved with an optimized detector, allowing a further decrease in the injected sample volume.

The separation efficiency of the glass device was also evaluated as a function of applied voltage, as shown in Figure

(28) Jorgenson, J. W.; Lukacs, K. D. *Anal. Chem.* **1981**, *53*, 1298.
(29) Huang, X.; Coleman, W. F.; Zare, R. N. *J. Chromatog.* **1989**, *480*, 95–110.
(30) Karger, B. L.; Snyder, L. R.; Horvath, C. *An Introduction to Separation Science*; J. Wiley and Sons: New York, 1973; pp 136–137.

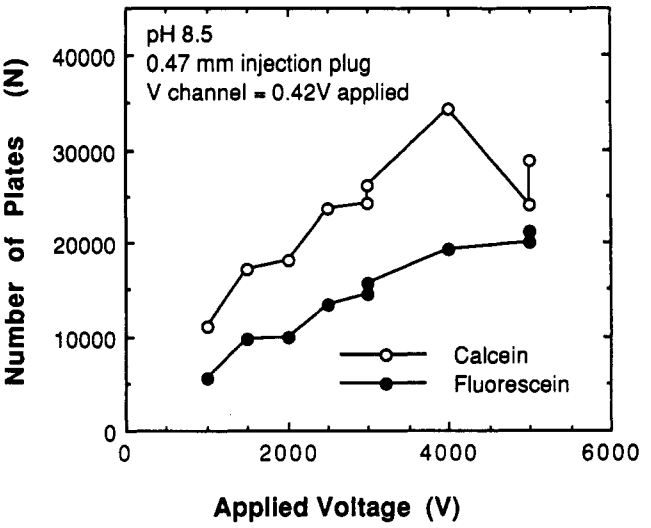

Figure 6. Plot of N versus the total applied voltage between reservoirs 1 and 3 for fluorescein (○) and calcein (●). The sample plug was about 0.47 mm long.

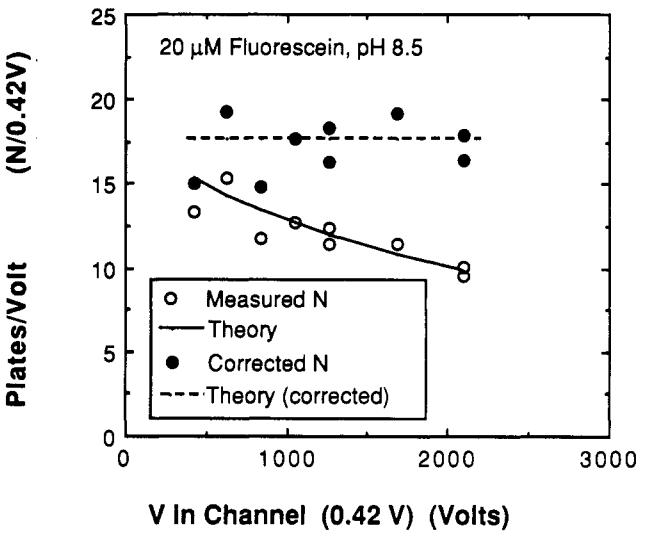

Figure 7. Plot of the number of plates per volt between the injection and detection points, $N/(0.42V_{ap})$, for the fluorescein data in Figure 6. The plates per volt corrected for band broadening introduced by the injector and detector is also shown. The lines are theoretical curves, as discussed in the text.

6. The potential between the injection point and the detector was 0.42 V_{ap}, and the injection plug length was estimated to be 0.47 mm. The efficiencies were fairly different for the two components of the sample, with a maximum number of plates of about 35 000 found for calcein.

To evaluate the possibility of wall interactions, the height equivalent to a theoretical plate, H, was evaluated experimentally and compared to theory. Band broadening in the capillary arises principally from longitudinal diffusion effects, as shown by eq 4,[29] where H_{diff} is the plate height due to

$$H_{diff} = 2Dt_m/d \quad (4)$$

longitudinal diffusion and D is the diffusion coefficient. In addition to diffusional broadening the injection plug length and the detector cell volume contribute to the overall variance, σ_{tot}^2:

$$\sigma_{tot}^2 = \sigma_{diff}^2 + \sigma_{det}^2 + \sigma_{inj}^2 + \sigma_{int}^2 \quad (5)$$

The diffusional variance, σ_{diff}^2, is given by $2Dt_m$, and σ_{det}^2 and σ_{inj}^2 will be given by $w^2/12$,[29,31] where w is the length of the detector cell or injected plug and a rectangular shape is assumed. Zare and co-workers[29] have suggested an additional interaction term, σ_{int}^2, should be included if the capillary walls interact with the analyte and lead to band broadening. They also indicate that, if this term is ignored when present, it will lead to an effective diffusion coefficient obtained from σ_{diff}^2 that differs from the true value. Thus, a comparison of D obtained from plotting H versus t_m with an independently determined value provides insight into the extent of analyte–wall interactions in a capillary.

Plots of H versus t_m for both fluorescein and calcein were linear over a range of V_{ap} from 1000 to 5000 V. Calcein data showed a slope of $(7.4 \pm 0.8) \times 10^{-7}$ cm/s and an intercept of $(1.3 \pm 0.2) \times 10^{-4}$ cm. The slope corresponds to a diffusion coefficient of $(2.4 \pm 0.3) \times 10^{-6}$ cm²/s for calcein in the pH 8.5 buffer. Fluorescein data gave a slope of $(1.02 \pm 0.07) \times 10^{-7}$ cm/s and an intercept of $(1.4 \pm 0.3) \times 10^{-4}$ cm; this gives a diffusion coefficient of $(3.3 \pm 0.2) \times 10^{-6}$ cm²/s. An independent measurement of $D = (3.4 \pm 0.3) \times 10^{-6}$ cm²/s for fluorescein in pH 8.5 buffer was obtained using a polarographic method.[26] Equation 4 predicts a zero intercept for a plot of H versus t, unless there is another source of broadening, such as indicated in eq 5. For these experiments the sample plug width was 0.047 cm and the detector length was approximately 0.09 cm. The value of the intercept in a plot of H versus t_m should be given by $(\sigma_{inj}^2 + \sigma_{det}^2)/d$. For the dimensions mentioned above this gives 1.3×10^{-4} cm, in agreement with the measured value of $(1.3–1.4) \times 10^{-4}$ cm. Consequently, all of the band broadening observed in the glass structure can be accounted for by eqs 4 and 5, excluding the σ_{int}^2 term. We conclude that the system behaves essentially ideally, with no wall interactions for the species studied.

Figure 7 shows how the number of plates per volt between the injection and detection points, $N/(0.42V_{ap})$, varied with the voltage between these points $(0.42V_{ap})$. A range of about 10–15 plates/V is seen for fluorescein, decreasing at higher applied V. Since μ and D were obtained experimentally for fluorescein, as was the extracolumn variance $(\sigma_{inj}^2 + \sigma_{det}^2)$, it is possible to calculate N by combining eqs 1, 4, and 5 to obtain eq 6. This expression, divided by $0.42V_{ap}$, is plotted

$$N = d^2\left[\frac{2DdL}{\mu(0.91V_{ap})} + \sigma_{inj}^2 + \sigma_{det}^2\right]^{-1} \quad (6)$$

as a solid line in Figure 7. The agreement shows that the decrease in $N/(0.42V_{ap})$ with V_{ap} arises from the contributions of extracolumn band broadening rather than joule heating or analyte–wall interactions. The number of plates due to the column alone, corrected for the detector cell and injection plug length contribution to H (1.4×10^{-4} cm), was estimated using eq 7, where N_{corr} is the corrected value and H is the

$$N_{corr} = \frac{d}{H - 1.4 \times 10^{-4}\ \text{cm}} \quad (7)$$

observed plate height in centimeters. The values of $N_{corr}/(0.42V_{ap})$ as a function of V_{ap} are shown in Figure 7. A theoretical curve calculated according to eq 6, neglecting the extracolumn contributions, is also plotted as a dashed line. These corrected values are in the range 15–20 plates/V and are comparable to typical results of about 20–25 plates/V reported for open tubular, fused-silica capillaries. In fact, the calcein dye shows somewhat higher values of 20–35 plates/V, after correction for band broadening due to the injector and detector lengths. These results indicate very reasonable performance from the prototype planar glass device, especially given the limitations of the detector design used.

(31) Sternberg, J. C. *Adv. Chromatog.* **1966**, *2*, 206–270.

CONCLUSIONS

To actually realize complex sample-handling and separation steps in an integrated, planar structure requires that a number of basic principles be shown to work in such systems. This study has examined and demonstrated the feasibility of using electroosmotic pumping to control flow in a manifold of flow channels without the use of valves. This is a significant aspect of the μ-TAS concept, and its realization demonstrates that more complex sample-handling steps such as those used in FIA can be achieved with this approach. That the flow rates are comparable to fused-silica capillaries shows that pumping rates will be predictable and that the glass substrate is a suitable material for this application.

Separation of samples is an equally important aspect of a μ-TAS device, and the present work shows that electrophoretic separation can be achieved on a planar substrate. The measured separation efficiency is quantitatively described by the expected theoretical relationship, indicating the device behaves essentially ideally. In fact, the efficiency expressed as the number of plates per volt is similar to that achieved with conventional open tubular, fused-silica capillaries. While 5000 V applied was translated into fields in the active part of the channel that did not exceed 2100 V, the data show that redesign of the device layout will easily increase this value. Manipulation of the channel geometry to control where the bulk of an applied potential drops was shown to be easily accomplished. Further, relatively high electric fields of 350 V/cm were obtained with no isolation of the contact leads, similar to the values typically used in conventional capillaries. Higher fields of at least 1800 V/cm can be sustained within the channels when the leads are isolated, and by using the appropriate channel geometry virtually all of this potential can be applied across the active portion of the channel. Overall, glass appears to be a satisfactory substrate for development of planar structures. It is compatible with both micromachining methods and electrophoresis.

The application of micromachining techniques to prepare miniaturized, 3-dimensional structures for chemical sensing and analysis is in its infancy. The present work suggests that relatively complex systems will be realized in the future that will compete with chemical sensors and with present benchtop analysis systems. Microstructures and capillaries, integrated detector systems, valveless switching of sample flow, and electroosmotic pumping are concepts that can be combined in a variety of ways to produce unique, miniaturized analytical systems. Such systems could lead to "laboratories on a chip" that offer rapid, sophisticated analyses in a mobile package that is free to leave the laboratory. The possibility of mass fabricating devices using integrated circuit and micromachining technologies may lead to low-cost systems with applications ranging from industrial process control to clinical analysis. However, considerable effort will be required to explore the many possibilities of the μ-TAS concept and micromachining technology and to establish their future impact on applications in chemical analysis.

ACKNOWLEDGMENT

We thank A. Bruno for assistance with the fluorescence detector and A. Paulus for measurements with the commercial CE instrumentation and for valuable discussions. D.J.H. thanks Ciba Geigy for the opportunity to work in their laboratories and partial support during his sabbatical leave. Z.F. acknowledges the Alberta Microelectronic Centre for a graduate fellowship.

RECEIVED for review January 3, 1992. Accepted May 21, 1992.